



Piperidinyl-2-phenethylamino inhibitors of DPP-IV for the treatment of Type 2 diabetes

John W. Benbow*, Kim A. Andrews, Jiri Aubrecht, David Beebe, David Boyer, Shawn Doran, Michael Homiski, Yu Hui, Kirk McPherson, Janice C. Parker, Judith Treadway, Maria VanVolkenberg, William J. Zembrowski

Pfizer Global Research and Development, Groton Laboratories, 558 Eastern Point Road, Groton, CT 06340, United States

ARTICLE INFO

Article history:

Received 21 January 2009

Revised 24 February 2009

Accepted 25 February 2009

Available online 28 February 2009

Keywords:

Dipeptidyl peptidase-IV

DPP-IV

Phenethylamine

ABSTRACT

A highly ligand efficient lead molecule was rapidly developed into a DPP-IV selective candidate series using focused small library synthesis. A significant hurdle for series advancement was genetic safety since some agents in this series impaired chromosome division that was detected using the in vitro micronucleus assay. A recently developed high-throughput imaging-based in vitro micronucleus assay enabled the identification of chemical space with a low probability of micronucleus activity. Advanced profiling of a subset within this space identified a compound with a clean safety profile, an acceptable human DPP-IV inhibition profile based on the rat PK/PD model and a projected human dose that was suitable for clinical development.

© 2009 Elsevier Ltd. All rights reserved.

An increasing incidence of obesity has, in part, fueled the rise in new Type 2 Diabetes Mellitus (TTDM) diagnoses and continues to make the treatment of TTDM a critical global health care issue.¹ Present pharmaceutical therapy fails to provide adequate glycemic control and many patients are unable to achieve their targeted plasma glucose levels through available regimens. Inhibition of the serine protease dipeptidyl peptidase-IV (DPP-IV) has recently emerged as an effective biological target for the treatment of TTDM.² Two of the targets for DPP-IV are the incretin hormones glucagon-like peptide-1 (GLP1) and gastrointestinal inhibitory peptide (GIP), bioactive molecules that are secreted by the gut in response to food intake.³ Binding of GLP1 to the pancreas and pancreatic β -cells leads to insulin secretion and results in enhanced glucose disposal. GLP1 has also been reported to provide benefits to the pancreas through improved beta cell function and possible regeneration.⁴ From a safety standpoint, DPP-IV inhibition offers a significantly reduced risk of hypoglycemia because the endogenous insulin secretagogue (GLP1) is generated only in response to a glucose stimulus. A first in class DPP-IV inhibitor Januvia® (MK-0431, **1**) has been approved and other agents are in review at the FDA [Galvus™ (LAF-237, **2**); Alogliptin (SYR-322, **3**)] (Fig. 1). We were interested in finding additional novel small molecular weight inhibitors of DPP-IV that lacked the 2-cyanopyrrolidide as a back-up to our clinical candidate, PF-00734200 (**4**). This account describes the discovery of a novel piperidinyl-2-phen-

ethylamino series of DPP-IV inhibitors and the tactics used to manage pre-clinical safety risks to identify promising clinical candidates.

The laboratory objective of the back-up effort was a once-a-day oral therapy that would provide $\geq 80\%$ inhibition of DPP-IV for at least 8 h in humans. Compounds would have demonstrated >100 -fold selectivity against DPP2 and DPP8 and have rat PK properties that would translate into acceptable human PK parameters. The successful candidate must also have no QTc prolongation risk, as judged by a 300x therapeutic index against hERG (hERG IC_{50} /DPP-IV $K_i \geq 300$) ($K_i = IC_{50}/1.66$) and a clean profile in the in vitro genetic toxicity assays (Bioluminescent Salmonella Assay and in vitro micronucleus assay).⁵

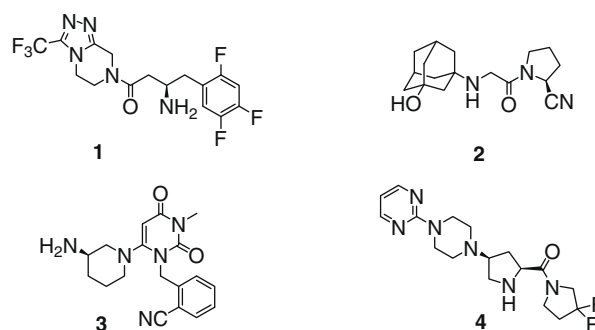


Figure 1. Advanced DPP-IV inhibitor clinical candidates.

* Corresponding author.

E-mail address: orgodoc@comcast.net (J.W. Benbow).

Table 1
DPP-IV inhibition of C1-substituted 1-amino-2-(2,4,5-trifluoro)phenylethanes, **5**



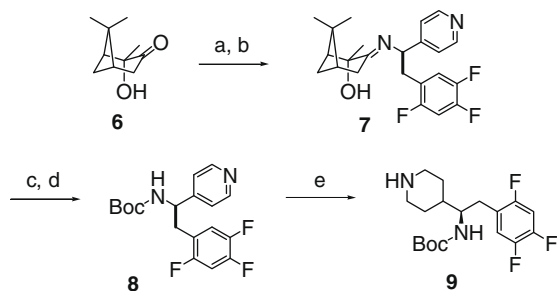
Compounds	R ¹	R ²	DPP-IV inhibition IC ₅₀ , μM ^a	Ligand efficiency (LE) ^b
5a	H	H	>30	
5b	<i>i</i> -Pr	H	1.93	0.52
5c	Cyclohexyl	H	3.58	0.41
5d	Cyclohexyl-CH ₂ -	H	>30	<0.32
5e	<i>t</i> -Bu	H	25.9	0.39
5f	-(CH ₂) ₄ -	H	>30	<0.39
5g	4-CH ₃ O ₂ CPh-	H	3.25	0.34
5h	1-(<i>R</i>)-4-CH ₃ O ₂ CPh-	H	1.42	0.36
5i	1-(<i>S</i>)-4-CH ₃ O ₂ CPh-	H	>30	<0.28
5j	1-(<i>R</i>)-4-Pyridyl	H	1.97	0.43
5k	1-(<i>R</i>)-4-Piperidinyl	H	0.272	0.50
5l	<i>N</i> -Boc-piperidin-4-yl	H	0.27	0.36

^a Values are means of three experiments.

^b Ligand efficiency is measured from the following equation: LE = -1.4 log K_i/# of heavy atoms. K_i was determined from the IC₅₀ values using the Cheng–Prusoff equation: K_i = IC₅₀/(1 + [S]/K_m) where [S] = 50 μM and K_m = 57 μM.

The 2,4,5-trifluorophenethylamino substructure was an established proline amide replacement in the S1 pocket and structural information suggested that the S2 pocket was sufficiently large and flexible enough to accommodate a variety of drug-like motifs.⁶ As part of a lead-hopping effort around the pharmacophore substructure, a series of simple phenethylamine derivatives were made and screened. While the un-substituted parent structure **5a** was an inefficient inhibitor of DPP-IV action, simple alkyl (**5b** and **c**) produced highly ligand efficient molecules (Table 1). A synthetic strategy using accessible chemical space was employed to probe the area directly outside of the S1 pocket and enabled the discovery of a viable, novel lead series. Substitution near the primary amine disrupted binding to the critical glutamate residues on the floor of S1 pocket: quaternary substitution alpha to the phenethylamine chain (**5e**), secondary nitrogen in the form of a saturated heterocycle (**5f**) or the extension of the alkyl substituent from the main backbone (**5d**) was not tolerated. However, non-polar, racemic aryl substitution **5g** on the ethyl chain was tolerated and asymmetric HPLC separation of the 4-methylbenzoate analogs established that the preferred amino stereochemistry was (*R*). The S2 pocket also tolerated basic polarity (4-pyridyl (**5j**) and 4-piperidinyl (**5k**)) and the *N*-Boc analog (**5l**) provided an opportunity to effectively explore this region of the binding site using a variety of functional groups that could modulate the physical chemical properties of the core.

An efficient route to the library-enabled template **9** was devised using the asymmetric alkylation method of Shioiri (Scheme 1).⁷ The commercially available 4-aminomethylpyridine was reacted



Scheme 1. Asymmetric route to (*R*)-1-(piperidin-4-yl)-1-amino-2-(2,4,5-trifluoro)phenylethane. Reagents and conditions: (a) 4-aminomethylpyridine, BF₃·Et₂O, PhCH₃; (b) *n*-BuLi, THF, <-20 °C then 2,4,5-F₃BnCl; (c) NH₂OH, EtOH, heat; (d) Boc₂O, 1,4-dioxane; (e) H₂, Pt₂O, EtOH, AcOH.

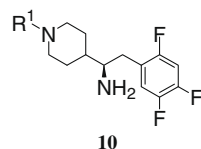
with (*S*)-hydroxypinanone **6** to form the corresponding imine and diastereoselective alkylation with 2,4,5-trifluorobenzyl chloride proceeded in good yield to afford **7** with excellent diastereoselectivity (>98% de). Removal of the imine through *trans*-oximation provided the primary amine intermediate that was readily converted into the *N*-Boc derivative **8**. Hydrogenation of the pyridine heterocycle (Pt₂O, AcOH) afforded the key piperidine intermediate **9** that could be recrystallized from EtOH to afford the *N*-Boc piperidine in good yield.

Having identified a suitable template, medium speed synthesis methods were used to produce a diverse set of analogs to probe the DPP selectivity SAR, generate benchmark data for in silico ADME modeling and to survey the behavior in the secondary safety screens. The 2-(2,4,5-trifluoro)phenethylamino moiety effectively delivered the required selectivity over the DPP8 isoform (IC₅₀ = 5–30 μM) regardless of the substitution elsewhere in the molecule. Selectivity over the DPP2 isoform could be achieved by modulating the potency against DPP-IV and DPP2 in tandem: piperidine-1-yl substituents with rotational flexibility such as amides, sulfonamides and alkyl chains improved DPP-IV inhibition and generally decreased the activity against DPP2. The DPP-IV IC₅₀ values in conjunction with the in vitro ADME screening data could be used to filter compounds for rat PK/PD experiments. Criteria used for selection were: DPP-IV IC₅₀ <100 nM; clearance in rat and human microsomes of <19 or <5 mg/mL/min, respectively, and Apical→Basal (AB) apparent permeability >10 cm⁻¹/s in MDCK cells with negligible efflux (BA/AB <3); single point dofetilide inhibition <20% at 10 μM compound. In addition, safety data was generated on a subset of analogs that indicated an unacceptable level of hERG inhibition and an increase incidence of micronuclei (aneugenic activity) (3/4) in the in vitro micronucleus assay.⁸ At this stage, an assessment of this series suggested that compounds with an acceptable selectivity profile and appropriate PK properties could be identified (Table 2).

Because not all of the compounds in this series were positive in the micronucleus assay, the activity was not believed to be specific to the pharmacophore. However, the usual low-throughput assay had insufficient capacity to handle the volume of samples needed to de-risk this chemical series in a timely manner; the microscopic scoring of the micronuclei is a laborious and time-consuming process. A recently developed image analysis algorithm for micronuclei scoring and implementation of automated microplate technologies enabled the testing up to forty compounds at a time.⁹ The ability

Table 2

DPP-IV inhibition, DPP2 selectivity, in vitro Human microsomal clearance and MDCK permeability of C1-substituted 1-amino-2-(2,4,5-trifluoro)phenylethane amides, **10**

**10**

Compd	R ¹	DPP-IV IC ₅₀ (nM)	DPP2 IC ₅₀ ^a (μM)	Human CL ^b (mL/min/kg)	MDCK AB ^c (10 ⁻⁶ s)
10a		35	11,100	<5.3	10.1
10b		26	10,200	<5.3	7.4
10c		19	9110	7.2	17.5

^a Values are means of three experiments.

^b Values represent the disappearance of compound from cultured human liver microsomes.

^c Values represent the apical to basal migration of compound in a Madin–Darby canine kidney cell line.

to screen a larger number of compounds using this technology enabled the identification of chemical sub-series with a predicted low-probability for chromosomal aberration (<20% positive). The first round of screening data demonstrated that various piperidine head-groups could be differentiated. Heteroatom-substituted indene amides (**10f and g**) attached through either the five- or six-membered ring were largely inactive (Table 3) as were aryl or alkyl sulfonamides, but the sulfonamides were not profiled further due to poorer DPP-IV inhibition and sub-par ADME properties. Amino-linked heteroaromatics, benzamide and benzylic substituents delivered positive results more frequently (≥50% positive) and work on these types of analogs was discontinued. A representative set of heteronaphthamide analogs (e.g., **10b**) demonstrated a 50% probability for chromosomal aberrations and work on these analogs was discontinued. A smaller set of heteroaryl amide analogs (e.g., **10c**) gave similar results and the set was expanded in the second submission. These data supported further investment in heteroatom-substituted indenamides and identified the six-membered heteroaromatic amide series as viable chemical space. The high-throughput micronucleus assay had enabled the identification of two chemical sub-series with a low probability of genetic toxicity within six weeks. The generation of this same data for 60 analogs using the manual micronucleus assay would have taken 4–5 months, a considerable savings in opportunity costs.

Table 3

In vitro CHO micronucleus screening results for different sub-series of phenethylaminopiperidiny DPP-IV inhibitors

Compound headgroup	Manual ^a INMN assay		1st imaging screen		2nd imaging screen		Total % Neg. (n)
	+	–	+	–	+	–	
Heteroaromatic	1		2	0			0 (3)
Benzamidoyl	1		3	0	1	4	50 (8)
Heteroatom-substituted indenamidoyl		1	2	10	0	3	88 (16)
Hetero-naphthamidoyl	1		4	5	0	1	55 (11)
Sulfonamidoyl			1	3			75 (4)
Hetero-arylamidoyl			2	3	0	9	86 (14)
Benzylic			3	1			25 (4)

^a Results are reported as positive (+) or negative (–) based on a reading of the amount of aberrant chromosomes after 24 h treatment of CHO cells with compound at varying concentrations.

Table 4

DPP-IV inhibition, DPP2 selectivity, safety and rat PK/PD of C1-substituted 1-amino-2-(2,4,5-trifluoro)phenylethanes

**10**

Compd	R ¹	DPP-IV IC ₅₀ (K _i) (nM)	DPP2 IC ₅₀ ^a (μM)	hERG IC ₅₀ ^b (μM)	Rat PK/PD ^c (h)
10d		18	>30	85	8–24
10e		22	>30	55	12–16
10f		27	10.8	59	>24
10g		4.0 (2.1)	16.8	18	>20

^a Values are means of three experiments.

^b For a description of the hERG patchclamp assay, please see: Fermini, B. and Fossa, A. A. *Nat. Rev.* **2003**, 2, 439.

^c Animals were dosed at 5 mg/kg, p.o. with methyl-cellulose solutions through oral gavage. Data reported shows the time that 50% inhibition of DPP-IV in plasma was achieved. Ranges represent intra animal variability in the DPP-IV inhibition profile.

The SAR of the heteroatom-substituted indenamidoyl and hetero-arylamidoyl sub-series was expanded through close-in analog synthesis. Optimal affinity for DPP-IV and the desired selectivity over the DPP2 isoform could be achieved by introducing small substituents *ortho*- to the amide carbonyl. Acceptable physical property space had been maintained throughout this effort and a small set of pre-candidates emerged that represented both chemical sub-series for profiling in the rat PK/PD model and the definitive safety assays (Table 4). These agents demonstrated an acceptable hERG window and all tested negative in the in vitro micronucleus assay.

The rat PK/PD profile for **10g** was sufficiently promising to advance this compound for a dog PK evaluation. The ADME data from these two species (rat and dog) allowed the projected human PK parameters to be calculated (Table 5). The human dose projection¹⁰ from modeling suggested that a 15 mg dose of **10g** would provide 80% inhibition of DPP-IV for 8 h and >50% inhibition for 16 h in humans.^{10,11}

In conclusion, the highly ligand efficient lead molecule **5k** was quickly developed into a candidate series using small focused library synthesis and a recently developed higher-throughput image analysis-based in vitro micronucleus screening assay. Ad-

Table 5
Pharmacokinetic data of **10g** from rat and dog and the projected human parameters

Species	CL _p ^c (ml/min/kg)	Vd _{ss} ^d (L/kg)	t _{1/2} ^e (h)	F (%)	f _u ^f
Rat ^a	18.0	2.2	5.09	70	49
Dog ^b	12.9	2.2	3.71	52	42
Human (Projected)	3.4	1.0	3.5	70	30

^a Rats (*n* = 2) were dosed with 1 mg/kg (i.v.) and 5 mg/kg (p.o.) in saline and 5% methyl cellulose, respectively.

^b Dogs (*n* = 2) were dosed with 1 mg/kg (i.v.) and 1 mg/kg (p.o.) in saline and 5% methyl cellulose, respectively.

^c Clearance of compound from plasma.

^d Volume of distribution calculated from the i.v. portion of the experiment.

^e Half-life was calculated from the i.v. portion of the experiment.

^f The unbound fraction of drug was measured using fresh plasma.

vanced profiling in the rat PK/PD model and subsequent human projections identified **10g** as having an acceptable human DPP-IV inhibition profile with a projected 15 mg/q.d. that was suitable for a drug development candidate.¹¹

References and notes

- (a) Flier, J. S. *Cell* **2004**, *116*, 337; (b) Hogan, P. et al *Diabetes Care* **2003**, *26*, 917.
- Pei, Z. *Curr. Opin. Drug Disc. Dev.* **2008**, *11*, 512.
- Flatt, P. R. et al *Front. Biosci.* **2008**, *13*, 3648.
- Drucker, D. J. *Endocrinology* **2003**, *144*, 5145.
- Bioluminescent Salmonella assay: (a) Aubrecht, J. et al *Mutagenesis* **2007**, *22*, 335; The in vitro micronucleus assay: (b) Sobol, Z. et al *Mutation Res.* **2007**, *633*, 80.
- Over the course of the DPP-IV project, over 30 crystal structure solutions were prepared, some of which have been published: (a) Wright, S. W. et al *Bioorg. Med. Chem. Lett.* **2007**, *17*, 5638; (b) Corbett, J. W. et al *Bioorg. Med. Chem. Lett.* **2007**, *17*, 6707.
- Irako, N. et al *Tetrahedron* **1995**, *51*, 12731.
- The in vitro micronucleus assay detects the presence of extra-nuclear chromatin (micronuclei) in cytoplasm as a consequence of either chromosome loss (aneugenicity) or chromosome breakage (clastogenicity). These effects can be differentiated via evaluating the kinetochore complex in micronuclei: Schuler, M. et al *Mutation Res.* **1997**, *392*, 81.
- The higher throughput in vitro micronucleus assay utilizes standard microplate technology, automated imaging using the Cellomics ArrayScan VTI (Thermo Fisher Scientific, Rockford, IL) and an image analysis scoring algorithm developed from an Image-Pro software platform (MediaCybernetics, Bethesda, MD). The results generated on set of test compounds using this assay compared favorably with those generated via the standard microscopic analysis.
- Human PK parameters were used to generate predicted plasma concentration versus time profiles at varying doses of **10g** (WinNonlin version 5.2, Pharsight Corp.). The projected human plasma concentration data was then used to predict the associated DPP-IV inhibition using the equation $[i = 1/(1 + K_i/I)]$, where 'i' is DPP-IV inhibition, 'K_i' is the value calculated from the in vitro EC₅₀ value, and 'I' is the unbound plasma concentration.
- A low dose (<50 mg q.d.) was desired to lower the risk of idiosyncratic toxicity in the clinic: Kalgutkar, A. S. et al *Exp. Rev. Clin. Pharmacol.* **2008**, *1*, 515.